CEBAF Program Advisory Committee Six (PAC6) Proposal Cover Sheet

This proposal must be received by close of business on April 5, 1993 at:

CEBAF

User Liaison Office

12000 Jefferson Avenue

Newport News, VA 23606

Proposal Title

POLARIZATION TRANSFER IN THE REACTION $^4He(\vec{e}, e'\vec{p})$ ^3H IN THE QUASI-ELASTIC SCATTERING REGION

Contact Person

Name: J. F. J. VAN DEN BRAND

Institution: UNIV. OF WISCONSIN

Address:

Address:

City, State ZIP/Country:

Phone: **FAX:**

E-Mail → BITnet: **Internet:**

If this proposal is based on a previously submitted proposal or letter-of-intent, give the number, title and date:

CEBAF Use Only

Receipt Date: 4/5/93 Log Number Assigned: PR 93-049

By: gp

Polarization Transfer in the Reaction ^{4}He($\vec{e}$,e'$\vec{p}$)^{3}H in the Quasi-elastic Scattering Region

Submitted by

J.F.J. van den Brand (Co-spokesman), H.J. Bulten, M. Bucholz
M. Miller, O. Unal and Z.L. Zhou
Department of Physics, University of Wisconsin, Madison
E-mail: JOELLE@WISCNUC
Ph.: (608) 262-9107
Fax.: (608) 262-3598

R. Ent (Co-spokesman)
Department of Physics, MIT, Cambridge

J. Gomez, J. LeRose, S. Nanda, A. Saha, and P.E. Ulmer (Co-spokesman)
Department of Physics, CEBAF, Newport News

E. Jans, and G. van der Steenhoven
NIKHEF-K, Amsterdam, The Netherlands

J.M. Finn, and C. Perdrisat
Department of Physics, College of William and Mary, Williamsburg

E. Brash, R. Gilman, C. Glashausser, G. Kumbartzki, R. Randsome, and P. Rutt
Rutgers University

Exp. No.	Description	Beam Hours	Energy	Current	D.F.
	^{4}He($\vec{e}$, e'$\vec{p}$)^{3}H	290	4 GeV	100 μA	100 %

ABSTRACT

We propose to perform a measurement of the polarization transfer coefficients in the reaction ^{4}He$(\vec{e},e'\vec{p})^3$H. This measurement will determine the dependence of these coefficients both as a function of the four-momentum transfer, over the range of 0.8 to 4 $(\mathrm{GeV/c})^2$ and as a function of missing momentum in the range of 0 to 250 MeV/c. The experiment exploits the 100 % duty factor polarized electron beam at CEBAF in combination with the proton polarimeter, which is presently being developed by a collaboration of the College of William and Mary, and Rutgers University. The combined knowledge of electron and proton spin enables a precise structure-function separation. The proposed experimental method allows a separation with small systematic error, as only one electron beam energy is used and the kinematical configuration is fixed. Recent calculations using a microscopic model predict that these spin-dependent structure functions are sensitive to the form factors of the proton bound in the dense ^{4}He nucleus. It is predicted that the proposed experimental method allows their extraction with minimal obscurance due to final-state interaction (FSI) and meson-exchange currents (MEC) effects. Measurement of the missing-momentum dependence of the polarization transfer coefficients will provide a stringent test of the ingredients in the description of the $(\vec{e},e'\vec{p})$ reaction mechanism.

We present estimates for the polarization transfer coefficients, D_{lt} and D_{ll}. It is shown that the coefficient D_{lt} can be determined to an accuracy of 1 - 7 %, and D_{ll} to an accuracy of 1 - 4 %. In the ratio of the coefficients D_{lt} and D_{ll}, which is sensitive to the bound proton form factor ratio G_M/G_E, part of the systematical uncertainties cancel. For the measurements probing the dependence of this ratio as a function of the four-momentum transfer, we expect better than 1 - 8 % statistical precision within the required beam time.

Table of Contents

I. Introduction

Knockout of a single proton from complex nuclei by high-energy electrons is generally assumed to proceed predominantly via a one-step reaction. In this description the virtual photon couples directly to the charge and the magnetic moment of the proton that is ejected and subsequently detected in coincidence with the scattered electron. Deviations of this impulse-approximation (IA) Ansatz have been observed in recent (e,e'p) experiments involving light- and medium-heavy nuclei[1-4]. Below the two-particle emission threshold significant deviations are found (up to 40 % for the ratio of backward to forward reduced cross sections). Several mechanisms have been proposed to account for the observed enhanced ratio of transverse and longitudinal response functions. Most of them are based on strong-interaction effects on the ejected proton[5-7] in the final state or on a conceptually novel idea concerning the identity of protons bound in a dense many-body quantum system, i.e. medium-modified nucleon form factors[8,9]. At this moment the precise explanation of the observations is still unclear.

All studies up to now used the conventional Rosenbluth technique for separating the structure functions. The measurements are extremely complicated as the experimental uncertainties are amplified due to the lever arm in the photon-polarization parameter. To keep the total systematical error within reasonable bounds the experimental parameters of the different kinematical configurations have to be carefully determined. This involves a precise calibration of the electron beam energies, the angles of both the scattered electron and the ejected proton, and the spectrometer acceptances.

We propose to study this deviation of the IA by using spin degrees of freedom. In this way the systematic error can be reduced as a structure function separation is performed for one kinematical configuration; all particle momentum vectors, $\mathbf{e}, \mathbf{e}'$ and $\mathbf{p_x}$ are fixed in the proposed experiment. Another advantage is that one is able to perform this separation at large values of the momentum transfer.

Advanced calculations show that the polarization transfer coefficients are sensitive to the form factors of the ejectile. In that case the obtained information will be much cleaner than in a regular longitudinal-transverse separation, as the main confusing contributions, due to the FSI and MEC effects, are expected to be small.

Measuring the polarization transfer coefficients as a function of the missing momentum further enables to study the validity of the IA, and provides a test on the description of the reaction $^4\mathrm{He}(\vec{e}, e'\vec{p})^3\mathrm{H}$. Employing the same experimental technique, we will be able to study the different contributions to the $(\vec{e}, e'\vec{p})$ reaction in more detail. In the absence of

PWIA-breaking processes the normal component of the proton polarization should be equal to zero. Therefore, this induced polarization component, which is helicity independent, is solely sensitive to interaction effects such as FSI and MEC effects, and may also provide a signature of the (e,e'n)(n,p) charge-exchange contribution[10].

In section II a more detailed scientific justification will be given for the proposed experiment. Details about the experimental setup, such as the proposed cryogenic target and the proton polarimeter, are given in section III. Count rates and run time estimates for the proposed kinematical settings are given in section IV.

II. Physics Motivation

2.1. Introduction

The interpretation of data obtained from inclusive and exclusive electron scattering experiments performed in the quasi-elastic scattering region is usually done assuming the impulse approximation. In the IA the nuclear current is, apart from modifications due to off-shell effects, given by the superposition of the individual free nucleon currents. In this framework it is possible to extract single-nucleon momentum probability distributions from the cross sections. However, in recent experiments evidence has been found supporting the idea that the IA may be inadequate. Among these is the detailed study of inclusive quasi-free electron scattering on a range of nuclei performed at MIT[11,12] and Saclay[13–15]. For all these nuclei, except ^{3}He and ^{4}He, a considerable amount of longitudinal strength is missing (up to 40 %). The transverse strength approximately agrees with what is expected.

In recent exclusive experiments[1–4] on ^{4}He, ^{6}Li, ^{12}C and ^{40}Ca an anomalous ratio of transverse and longitudinal response functions has been observed. In the (e,e'p) reaction the kinematics of the initial nucleon can be fixed and therefore, contrary to the inclusive experiments, scattering from a nucleon having a defined binding energy and initial momentum is selected. In this way one is far less dependent on nuclear structure calculations to study the validity of the IA. From the ratio of separated structure functions the ratio R_G has been formed, which is shown in Fig. 2.1 for ^{6}Li, ^{12}C and ^{40}Ca.

R_G has been interpreted as the ratio of magnetic and charge form factors for a bound proton. The ratio R_G represents at $Q^2 = 0$, in the case of a free proton, its magnetic moment $\mu_p = 2.79$ nm. The figure shows significant deviations from the value for a free proton and this has been interpreted as a signature of modifications of the spinors, current operators or nucleon form factors by the nuclear medium. The possible modification of the virtual-photon proton coupling may be explained by relativistic mean-field theories and QCD-inspired theories through the changes of the nucleon spinors and current operators. Results of a calculation[16] using a two-phase model consisting of a quark core surrounded by a pion cloud show that at nuclear-matter densities the proton form factors should not differ significantly from the free values. This is due to a cancellation between an enhancement of the charge radius by the polarization of the pion cloud which is masked by a Pauli blocking effect.

It has been argued by many authors that before considering such explanations one must be extremely cautious with the treatment of reaction-mechanism effects. It is well known that one has to incorporate correction factors associated with FSI and MEC effects for a complete description of the spin-averaged (e,e'p) cross section. The commonly applied

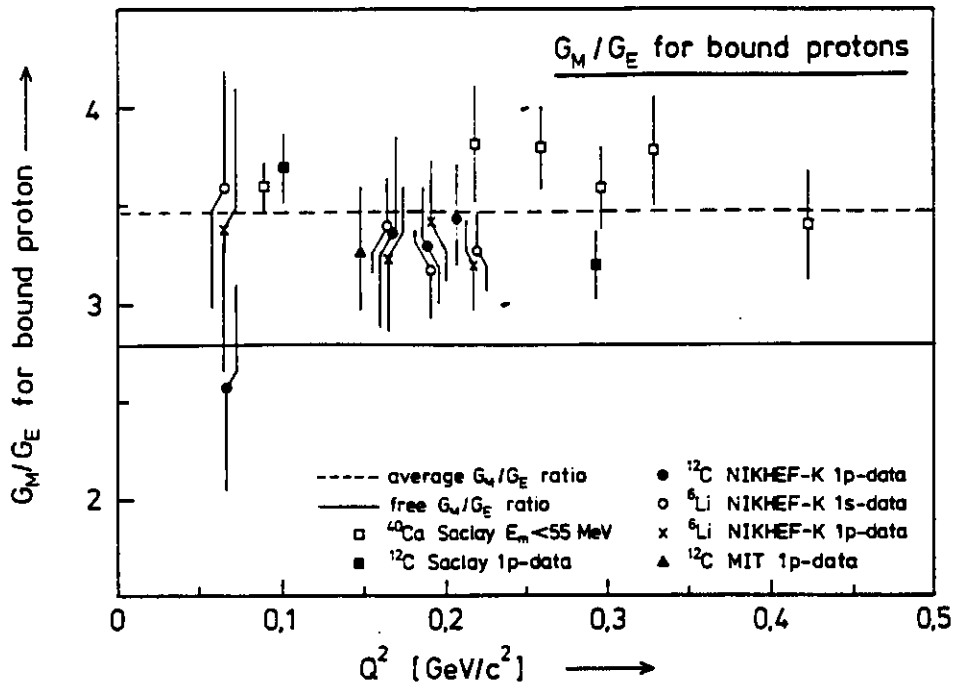

Figure 2.1. *R_G or ratio of form factors of a bound proton as a function of the four-momentum squared for exclusive quasi-elastic experiments on ^6Li, ^{12}C and ^{40}Ca. The results of MIT[3], NIKHEF[1] and Saclay[2] are displayed.*

DWIA treatment[17] of the FSI effects through a local optical potential that describes elastic proton-nucleus scattering may be inadequate. Alternative explanations of the experimental observations have been given in the Dirac distorted-wave impulse approximation[18,19] through a reduction of the longitudinal structure function by coupling to virtual negative-energy states. Some authors[6,7] argue that especially the spin-orbit field is responsible for the relative enhancement of the transverse part of the cross section.

Apparently, the effects of a possible medium modification of the virtual photon-proton coupling are so intertwined with reaction mechanism effects as FSI and MEC, that the recently performed (e,e'p) studies do not permit a clear interpretation. We therefore propose a study of the electromagnetic properties of the bound proton using spin degrees of freedom. Calculations indicate that this method largely eliminates the influence of reaction-mechanism effects on the extracted form factors.

The ^{4}He atomic nucleus is an ideal candidate for such a study of the interaction between the electron and the bound proton. The nuclear structure of ^{4}He is relatively simple and various results of recent four-body calculations are available[20,21]. If the electromagnetic properties of the proton change when it is embedded in the nuclear medium, then significant effects, if any, may be expected for this nucleus due to its high density. The

signature of these effects is expected to become experimentally observable, because advanced microscopic calculations, including FSI and MEC effects, have become possible for the ^{4}He(e,e'p)^{3}H reaction.

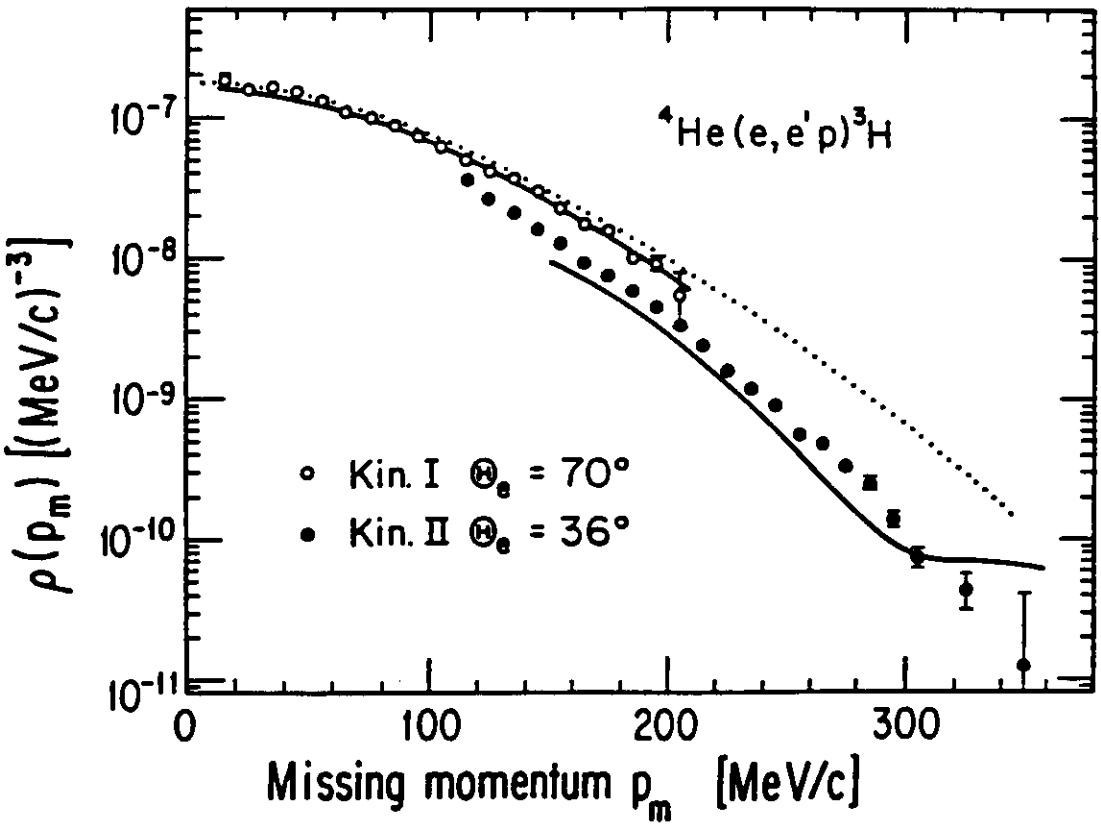

Figure 2.2. *Proton momentum distribution[22] for the two-body breakup of ^{4}He. The error bars include the statistical error only. The dotted curve represents a PWIA calculation[20] for the Urbana NN potential. The solid curves represent the results of the microscopic calculations taking FSI, charge-exchange and MEC effects into account[25].*

Experimental results obtained[22] in the reaction ^{4}He(e,e'p)^{3}H showed in first instance a dramatic (40 %) breakdown of the distorted wave impulse approximation with inclusion of charge exchange through a coupled-channels calculation. Additional data[23,24] obtained in both (anti-) parallel and perpendicular kinematical configurations were taken in order to study the observed breakdown in more detail. These kinematics (at fixed value of missing energy and missing momentum) were specially selected in order to probe the different

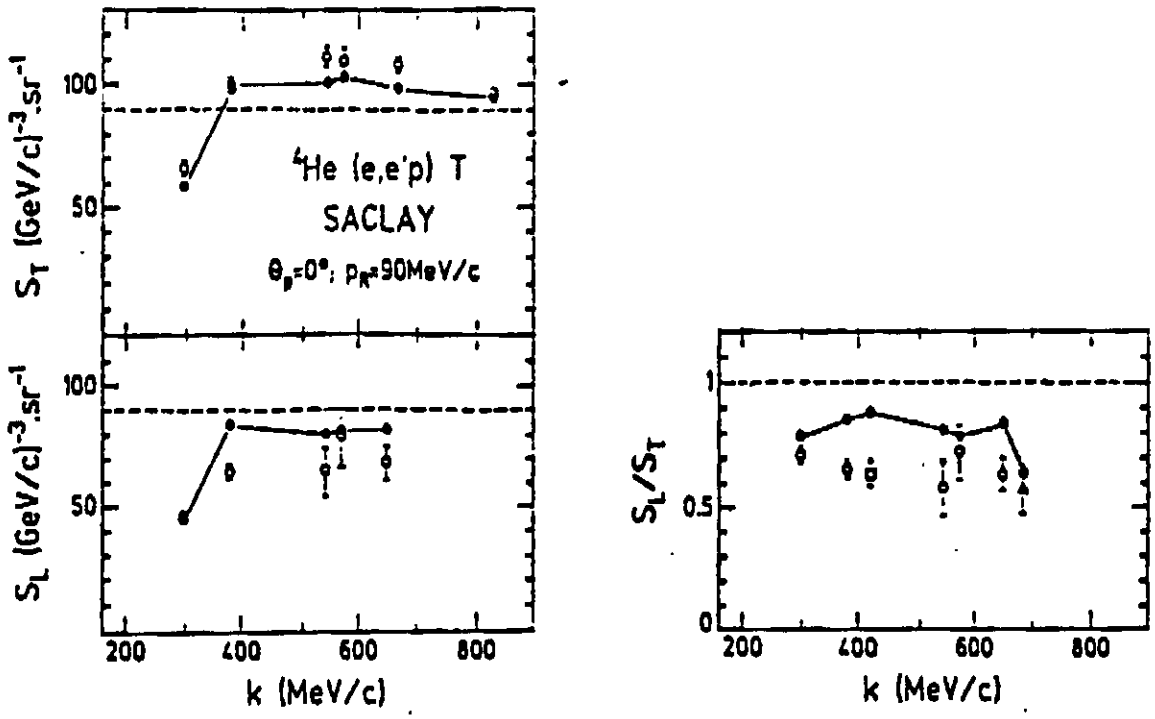

Figure 2.3. *The ratio of uncorrected (open symbols) and corrected (closed symbols) experimental*[4] *spectral functions, S_T and S_L, versus momentum transfer.*

contributions of the (e,e'p) reaction mechanism. The calculations include effects due to proton rescattering, the (e,e'n)(n,p) charge-exchange process, and meson-exchange currents. With this microscopic model the momentum density distribution for the two-body disintegration, shown in Fig. 2.2, is described better than 20 %. Also the experimentally observed dependence of the five-fold differential cross section on the total hadronic kinetic energy was described better than 20 %. We think that this agreement is rather impressive when one considers that these data go from the low-ω side to the high-ω side of the quasi-elastic peak. We further would like to remark that the description of the data on top of the quasi-elastic peak (Kin. 1 of Fig. 2.2) is almost perfect.

The structure functions have been separated in an experiment performed at Saclay[4] for the reaction ^{4}He(e,e'p)^{3}H in parallel kinematics. The ratio of uncorrected (open symbols) and corrected (closed symbols) experimental spectral functions, S_T and S_L, versus momentum transfer are shown in Fig. 2.3. Deviations up to 35 % from the IA are reported, even after correcting the data for FSI and MEC effects using the results of the microscopic model. The transverse structure function is assumed to be well described at the highest momentum transfer, whereas a suppression is observed in the longitudinal strength.

To clarify whether the observed deviations are due to more or less trivial reac-

tion mechanism effects or represent signals of a more fundamental nature we propose a ^{4}He$(\vec{e}, e'\vec{p})^3$H experiment, expected to be almost free of FSI effects and therefore sensitive to the ratio of G_M/G_E. At these high values of the momentum transfer a polarization transfer experiment is in our opinion the best way to test the validity of the Impulse Approximation. Next to this, in a polarization transfer experiment one can also test whether a possible experimental discrepancy with respect to the impulse approximation is a function of the missing momentum.

2.2. Formalism

The experiment involves the measurement of the three components of the proton polarization after being scattered quasi-elastically by the incident longitudinally polarized electron. The coordinate system used in describing the $(\vec{e}, e'\vec{p})$ reaction is outlined in Fig. 2.4.

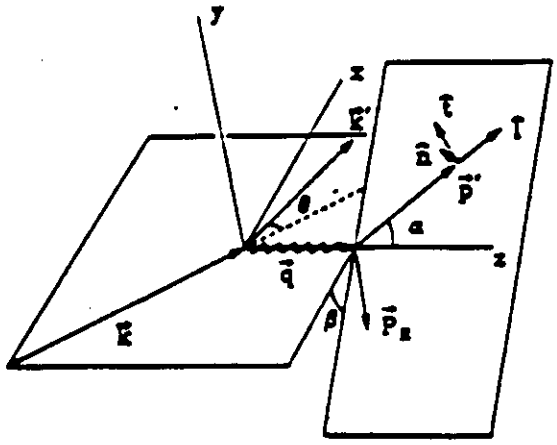

Figure 2.4. *The coordinate system and the various kinematical quantities.*

The differential cross section for this reaction can be written as[26]:

$$\begin{aligned}\frac{d^3\sigma}{dk'_0 d\Omega_{k'} d\Omega_{p'}}|_{h,s'} = \frac{m_p|\mathbf{p}'|}{2(2\pi)^3}\sigma_M[&V_L(R_L + R_L^n S_n) + V_T(R_T + R_T^n S_n) \\ &+ V_{TT}[(R_{TT} + R_{TT}^n S_n)cos2\beta + (R_{TT}^l S_l + R_{TT}^t S_t)sin2\beta] \\ &+ V_{LT}[(R_{LT} + R_{LT}^n S_n)cos\beta + (R_{LT}^l S_l + R_{LT}^t S_t)sin\beta] \\ &+ hV_{LT'}[(R_{LT'} + R_{LT'}^n S_n)sin\beta + (R_{LT'}^l S_l + R_{LT'}^t S_t)cos\beta] \\ &+ hV_{TT'}(R_{TT'}^l S_l + R_{TT'}^t S_t)],\end{aligned} \tag{2.1}$$

where k_0 (k_0') is the energy of the incident (scattered) electron, h is the incident electron helicity and σ_M is the Mott cross section. The kinematic factors are defined as:

$$\begin{aligned} V_L &= \frac{Q^4}{\mathbf{q}^4} \\ V_T &= \frac{Q^2}{2\mathbf{q}^2} + \tan^2\frac{\theta_e}{2} \\ V_{TT} &= \frac{Q^2}{2\mathbf{q}^2} \\ V_{LT} &= \frac{Q^2}{\mathbf{q}^2}\sqrt{\frac{Q^2}{\mathbf{q}^2} + \tan^2\frac{\theta_e}{2}} \\ V_{LT'} &= \frac{Q^2}{\mathbf{q}^2}\tan\frac{\theta_e}{2} \\ V_{TT'} &= \tan\frac{\theta_e}{2}\sqrt{\frac{Q^2}{\mathbf{q}^2} + \tan^2\frac{\theta_e}{2}}. \end{aligned} \tag{2.2}$$

Here $\mathbf{q}^2 = Q^2 + \omega^2$ in conventional notation. Given the coordinate system shown in Fig. 2.4, with unit vectors $\mathbf{n}$, $\mathbf{l}$ and $\mathbf{t}$, defined by choosing $\mathbf{l}$ parallel to the proton momentum, $\mathbf{n} = (\mathbf{q} \times \mathbf{l})/|\mathbf{q} \times \mathbf{l}|$ and $\mathbf{t} = \mathbf{n} \times \mathbf{l}$, the projection of the spin unit vector onto these basis vectors can be defined as:

$$S_n = \mathbf{n} \cdot \mathbf{s}_R', \; S_l = \mathbf{l} \cdot \mathbf{s}_R', \text{ and } S_t = \mathbf{t} \cdot \mathbf{s}_R'. \tag{2.3}$$

When choosing parallel kinematics only three spin-dependent structure functions survive: R_{LT}^n, $R_{LT'}^t$ and $R_{TT'}^l$, which determine the transverse component normal to the scattering plane, transverse component in the scattering plane, and the longitudinal component of the polarization vector of the ejected proton. The normal component, p_y^0, is helicity independent and vanishes in PWIA. The transverse component of the recoil polarization, p_x', which is located in the scattering plane is in PWIA related to the electron beam helicity, h, as:

$$p_x' = hD_{lt}. \tag{2.4}$$

The longitudinal component is given by:

$$p_z' = hD_{ll}. \tag{2.5}$$

In PWIA the polarization transfer coefficients D_{lt} and D_{ll} can be expressed[28] in terms of the nucleon form factors G_E and G_M:

$$I_0 D_{lt} = -2\sqrt{(\tau(1+\tau)}G_M G_E \tan\theta_e/2$$

$$I_0 D_{ll} = \frac{k_0 + k_0'}{m_p}\sqrt{(\tau(1+\tau)}G_M^2 \tan^2\theta_e/2 \tag{2.6}$$

$$I_0 = G_E^2 + \tau G_M^2[1 + 2(1+\tau)\tan^2\theta_e/2],$$

here $\tau = Q^2/4m_p$. It is seen that a form factor ratio R_P can be formed from the proton polarization components p_z' and p_x' and is given by:

$$R_P = -\frac{2m_p}{(k_0 + k_0')\tan\theta_e/2}\frac{p_z'}{p_x'} = \frac{G_M}{G_E}. \tag{2.7}$$

where R_P does not involve knowledge of the electron polarization, and the last equality is only true in PWIA. The systematic error in this ratio is expected to be small as only the accuracy of the incident and scattered electron energies, the scattering angle, and the spin precession angle enter.

The spin vector of the proton is measured in the polarimeter after it is momentum analyzed in the 4 GeV/c proton spectrometer. Contrary to both the normal and the longitudinal spin components, the sideways component does not precess (in first order) in the magnetic field of the spectrometer. The polarimeter coordinate system is defined as follows: X axis is along the momentum dispersion direction, Y axis is normal to the bend plane and Z axis is along the proton momentum. The polarization components after precession by an angle χ through the 4 GeV/c proton spectrometer are given by:

$$\begin{aligned} p_X &= p_y^0 cos\chi + p_z' sin\chi \\ p_Y &= p_x' \\ p_Z &= -p_y^0 sin\chi + p_z' cos\chi. \end{aligned} \tag{2.8}$$

The precession angle is given by:

$$\chi = \frac{g-2}{2}\gamma\Omega_B, \tag{2.9}$$

where g is the gyromagnetic ratio of the proton (5.586), γ is the Lorentz factor and Ω_B is the total bend angle in the proton spectrometer (for the central ray $\Omega_B = 45°$).

The focal-plane polarimeter determines therefore p_x' and a combination of longitudinal and normal components, p_z' and p_y^0. The normal component will be separated from p_z' using its independence of the electron helicity. However, for the large momentum transfer chosen in this experiment, and especially for small recoil momenta, p_y^0 is expected to be small.

2.3. Estimates for the Polarization Transfer Coefficients

For the present reaction the Coulomb distortion of the electron waves is negligible and one has the advantageous situation that the corrections for FSI effects can be applied either in a phenomenological manner[22,27] or on the basis of a microscopic theory. It has been shown in a recent ^{4}He(e,e'p)^{3}H experiment[24], where strong deviations from PWIA were observed, that the data cannot be explained by rescattering and charge-exchange effects when calculated in DWIA with a phenomenological local optical potential and extended with a coupled-channels approach (CCIA). A much improved description of the data can be obtained with a theoretical model[25,28] that has been already successfully applied to (e,e'p) results obtained on ^{2}H and ^{3}He. This microscopic model has been extended to the ^{4}He nucleus[29,30] and will be used in this section to present estimates for the polarization transfer coefficients.

The microscopic calculation for the ^{4}He nucleus uses the correlated bound-state wave function for the four-body system[20] obtained with the variational Monte-Carlo (VMC) method. In the theoretical description of the (e,e'p) reaction a diagrammatic expansion of the amplitude is made into a number of presumably dominant subamplitudes. For the current operator its non-relativistic reduction including terms of order $1/M_p^3$ is used. The spin-orbit term $\sigma \times \mathrm{p}$ and the Darwin-Foldy term $(1 + \mathrm{q}^2/8\mathrm{M}_\mathrm{p}^2)$ in the time component of the current operator are retained. The final-state wave function is fully anti-symmetrized and at the $\gamma - (A-1)$ vertex the free ^{3}H form factors[31] are used. The actual FSI contribution is treated in the single nucleon-nucleon (NN) rescattering approximation. This is accomplished by expanding the NN scattering amplitude in terms of the S, P and D scattering matrix elements. In the calculation the active nucleon pair can be in an isospin T = 0 or T = 1 state. The various overlaps with the ^{4}He nucleus for the angular momentum states under consideration are calculated up to 6 fm^{-1}. Furthermore, the meson-exchange amplitude is added coherently to the other amplitudes. Active nucleon pairs with isospin T = 0 and T = 1 are taken into account and S and D scattering states are allowed for. The calculation includes the exchange of both π and ρ mesons. The diagrams corresponding to the nucleon Born terms are included through the wave functions used.

In Fig. 2.5 the predicted longitudinal and transverse polarization components of the ejected proton are shown versus missing momentum. The kinematics used in the calculation are similar to those of the proposed experiment (kinematics 1 and 2) and therefore the results of the microscopic calculation may be used as a guideline. It is seen that for p'_x and p'_z the deviations from PWIA due to charge-exchange, FSI and MEC effects are negligible for missing momenta below 300 MeV/c. The component p^0_y

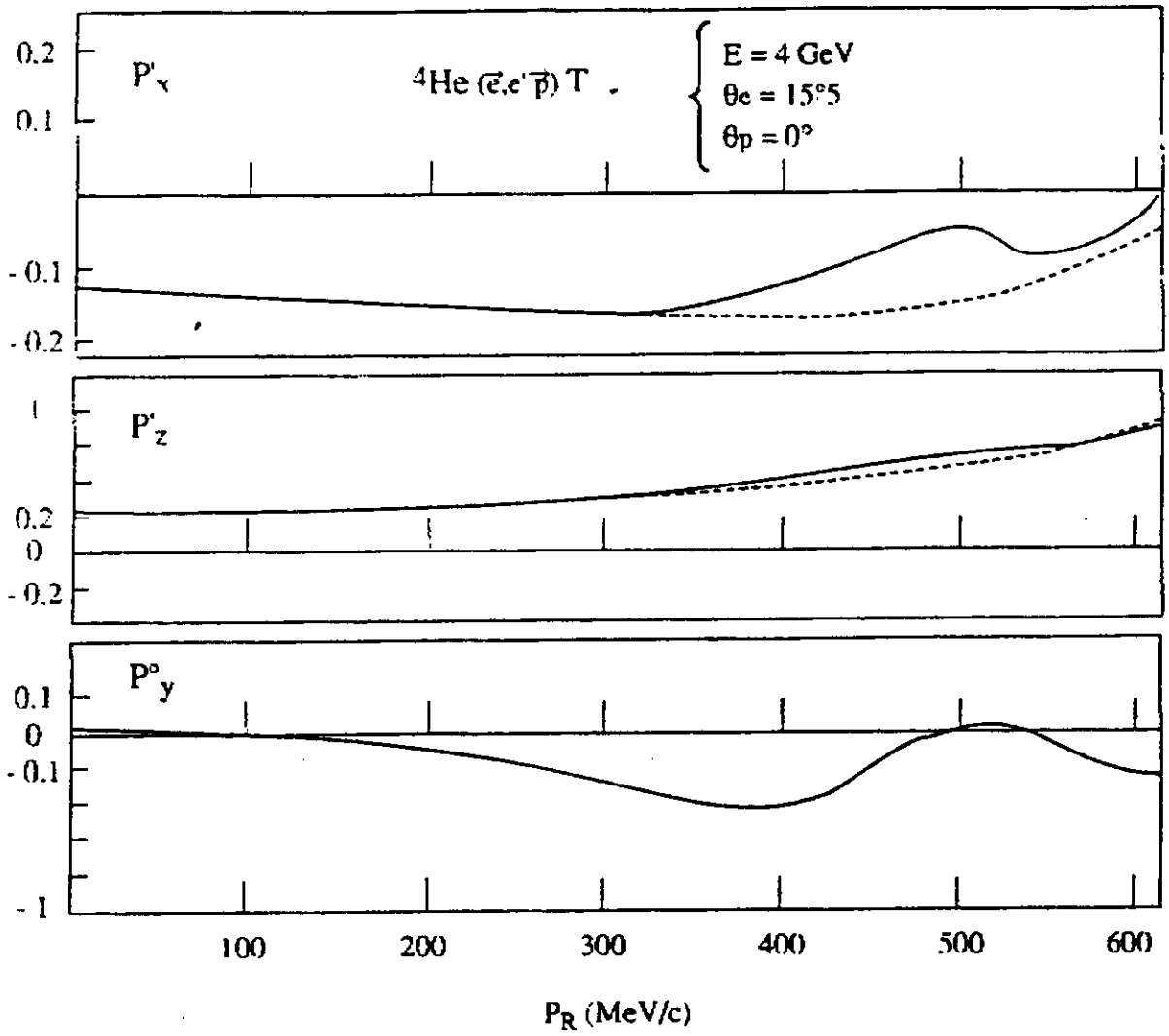

Figure 2.5. *The spin-transfer polarization p'_x, p'_z, and p^0_y of the reaction $^4He(\vec{e},e'\vec{p})^3H$ calculated by Laget[32]. The dashed curve is the PWIA prediction, and the solid curve represents the results of the calculation including FSI and MEC effects.*

for this kinematical setting increases with increasing missing momenta. The results of the calculation suggest that a measurement of the spin vector of the ejected proton yields information on the form factors of the bound proton. As shown in the figure the method is expected to be extremely insensitive to FSI and MEC effects.

III. The Experiment

3.1 Introduction

The experiment is proposed for the CEBAF electron-scattering facility using the Hall A spectrometers. An incident polarized electron beam with 100 % duty factor and an energy of 4 GeV will be used. At one value of the incident electron energy 4 measurements will be performed at four-momentum transfer values Q^2 = 0.8, 1.5, 3.0, and 4.0 $(GeV/c)^2$. We will map out the dependence of the polarization transfer coefficients as a function of the missing momentum, up to a value of 250 MeV/c. In the kinematics the experimental phase space will be centered at the missing-energy value of E_m = 20 MeV. The outgoing proton kinetic energy will vary between 0.43 GeV and 2.13 GeV. The coincidence data will be expressed as five-fold differential cross sections. For this purpose the data will be integrated over the missing-energy variable from 16 MeV to 24 MeV. In this way contributions from the three and four-body breakup channels are excluded. The anticipated missing-energy resolution is estimated at approximately 1 MeV. This requires the use of the high-resolution spectrometers available in Hall A.

The product of target thickness and the solid angle of the electron spectrometer will be determined by comparing elastic electron scattering cross sections with the results of phase-shift calculations using ground-state charge distribution parameters from the literature[33]. The target thickness may vary as a function of the dissipated power; its value at the coincidence setting will be related to the elastic electron scattering measurement by use of the corresponding proton singles rates.

The coincidence detection efficiency will be calibrated with the reaction ^{1}H(e,e'p). The total coincidence yield will be corrected for accidentals and weighed by the detection volume calculated with a Monte Carlo simulation, taking the angular acceptance of the spectrometers as a function of the vertex position into account. The comparison of the distribution of the simulated and the experimental accidentals will be used as a stringent consistency check. During the actual experiment the coincidence yield as a function of the incident electron beam position will be used as a check on the mutual alignment of the spectrometers, beam and target cell.

3.2 The cryogenic gas target

A cryogenic gas target is being developed by the Hall A collaboration. The ^{4}He gas target will be operated at a temperature of 10 K and a pressure of 70 atm. The corresponding target density amounts to 0.17 g·cm^{-3}. The LH_2 target, needed for calibration

purposes, will operate at 20 K and a pressure of 17 atm, necessary in order to suppress macro bubble formation. A description of the target system can be found in reference[34]. The target cells will have a length of 10 cm and can operate with beam currents up to 150 μA. The design value for the maximum cooling power amounts to 1 kW. For the proposed experiment we assume a beam current of 100 μA and consequently a moderate level of power dissipation ($<$ 500 W). The resulting luminosity amounts to 1.6×10^{38} e^-atoms $cm^{-2}s^{-1}$.

3.3 The focal-plane proton polarimeter

The focal-plane proton polarimeter for the 4 GeV/c proton spectrometer in Hall A is being developed by the Hall A collaboration. A full description of this polarimeter can be found elsewhere[34]. The design is based on existing technology and is similar to polarimeters already in use at LAMPF, IUCF, TRIUMF, and SATURNE. The design uses a graphite analyzer preceeded and followed by a series of straw drift chambers.

IV. Count-Rate and Running-Time Estimates

4.1 Kinematics

We propose to measure the ratio p'_z/p'_x. The polarimeter only determines p'_x and a combination of p^0_y and p'_z. The latter two contributions can be separated through the use of the electron helicity. The dependence on missing momentum will be measured up to 250 MeV/c within each kinematical setting.

The high momentum transfer values chosen for this experiment, and also the measurements up to high values of the missing momentum, should enable us to distinguish between any FSI effects and deviations of the impulse approximation. The kinematics are given in Table 1. The incident electron energy is chosen to be 4 GeV.

4.2 Count Rate Estimates

We have assumed the following spectrometer acceptances: 10 % in momentum and a solid angle of 7.8 msr. The polarimeter acceptance for second-scattering azimuthal angles completely covers the total momentum acceptance. As both spectrometers will see the total length (10 cm) of the extended target, a target thickness of 1.7 g·cm^{-2} has been used in the estimates. The center of the missing-energy acceptance will be kept at 20 MeV, which corresponds to a measurement of the two-body disintegration channel.

The coincidence count rate N_C is calculated from the five-fold differential cross section, the beam current, the target thickness, and the angular and momentum acceptances. The coincidence cross section for the discrete transition is given in PWIA by:

$$\frac{d^5\sigma}{dEd\Omega_e d\Omega_x} = \int_{\Delta E_m} \frac{d^6\sigma}{dE_e dT_x d\Omega_e d\Omega_x} \frac{\partial T_x}{\partial E_m} dE_m = \frac{E_x|\mathbf{p_x}|}{1 - \frac{E_x}{E_{A-1}} \frac{\mathbf{P_{A-1}}\cdot\mathbf{p_x}}{\mathbf{p_x^2}}} \sigma_{ep}\rho(|\mathbf{p_m}|). \quad (4.1)$$

Here $\rho(|\mathbf{p_m}|)$ is the single-particle momentum distribution and for σ_{ep} we used the off-shell electron-proton cross section description σ^1_{cc} by De Forest[35].

To determine the expected count rates we used a Monte Carlo code which generates events within the experimental phase space. The events are weighted using the appropriate kinematical factors and the off-shell e-p cross section using the CC1 prescription. A value for the spectral function S(E_m,$|\mathbf{p_m}|$) was taken from earlier data (see Fig. 2.2). Coincidence rates are given in Table 2, assuming an average current of 100 μA. No missing-momentum cuts have been applied. The table also shows the various singles rates. The electron singles rates have been calculated by adding the inclusive quasi-elastic scattering contribution to the Fermi-smeared deep-inelastic contribution. The (e,π^-) rates have been obtained with

the code EPC[36] and it can be seen that a sufficient rejection factor can be obtained with the Čerenkov and shower counters. The hadron singles rates have been obtained for (e,p) and (e,π^+) and have been calculated from a parametrization of measurements with incident bremstrahlung photons. The accidental rates are small in all kinematics. Significant improvement in the real-to-accidental ratio could be obtained by applying a missing-energy cut and a cut on the correlated vertex position. The latter cut alone is expected to improved R/A by at least an order of magnitude.

To calculate the statistical precision only those coincidence events which scatter usefully in the focal-plane polarimeter should be considered. The cross section for scattering a polarized electron from an unpolarized proton followed by a second scattering of the outgoing polarized proton from an analyzer is (for parallel kinematics):

$$\sigma = \sigma_0[1 + p'_x A_y sin\phi_2 + (p^0_y cos\chi + p'_z sin\chi)A_y cos\phi_2], \tag{4.2}$$

where ϕ_2 is the azimuthal angle of the secondary scattering, A_y is the analyzing power, σ_0 is the unpolarized cross section and χ is the precession angle in the proton spectrometer. By measuring the ϕ_2 distribution in the polarimeter one can disentangle the polarization component p'_x from the other polarization component, which is a combination of p^0_y and p'_z. The statistical uncertainty in either polarization component is:

$$\Delta p_i = \frac{\pi}{2\bar{A}_y}\sqrt{\frac{1}{fN}}, \tag{4.3}$$

where A_y is the analyzing power averaged over an angular cone for which A_y is substantially different than zero, f is the fraction of events that scatter into this cone and N is the total number of events detected in the spectrometer focal plane.

Shown in Table 3 are the assumed polarimeter parameters for each kinematics. Table 4 shows the run times.

4.3 Systematical Uncertainties

The excellent intrinsic resolution of the Hall A spectrometers will allow good control of the systematical accuracy of the proposed experiment. The two-body disintegration channel can be clearly separated from the continuum channels. As we will measure a p'_z/p'_x ratio for fixed kinematics, the systematical uncertainties are not very dependent on the missing-momentum resolution of the hall A spectrometer set-up. The determination of the average missing-momentum value for conventional longitudinal-transverse separation measurements, necessary because one has to measure at different kinematical situations,

will not influence this experiment. As the missing momentum dependence of p'_x and p'_z is somewhat different, some uncertainty will still be caused by the alignment of the spectrometers and the intrinsic resolutions of both spectrometers, but we estimate these effects to be small, and at least better than 1 % in the ratio.

A further systematical uncertainty appearing in the measurement of the ratio p'_z/p'_x will be the uncertainty in the precession angle χ in the proton spectrometer. Since it is the average precession angle which is important, it can be precisely determined from the centroid of a distribution with very high statistics.

The systematical uncertainties in the measurements of the polarization transfer coefficients itself consist mainly of uncertainties in target thickness, polarimeter, electron polarization, and intrinsic resolutions. The target thickness will be monitored by the proton singles rates, and we expect to achieve in this way a relative uncertainty of better than 1 %. The systematical uncertainty of the proton polarimeter is caused by uncertainties in the analyzing power A_y, and, as mentioned already before, the uncertainty in the average value of the precession angle χ. These uncertainties will be empirically determined by measurements of this polarimeter in Experiments 89-014, 89-028, and 91-006. The uncertainties caused by the alignment of the spectrometers and the intrinsic resolutions will appear more pronouncedly in the determination of the separate polarization transfer coefficients. We estimate them to be more or less equal as they appear in standard (e,e'p) experiments.

4.4 Beam Time Request

The total beam time required is 290 hours, including 50 hours for setting up and testing the experimental apparatus (see Table 5). The intended measurements will give an accurate experimental value of the ratio p'_z/p'_x with a statistical uncertainty of about 1, 2, 3, and 8 %, for Q^2 of 0.8, 1.5, 3, and 4 $(GeV/c)^2$, respectively. The estimate of this uncertainty is partly dependent on the model used to estimate the cross section and polarization transfer coefficients for the $^4He(\vec{e}, e'\vec{p})^3H$ reaction.

Combined with earlier data we will obtain by this experiment fundamental information on the dense ^{4}He nucleus. The advantage in determining the ratio of p'_z/p'_x in this way is that reaction-mechanism effects and the systematical uncertainties are minimized.

Table 1. Kinematics for the proposed ^{4}He$(\vec{e},e'\vec{p})^3$H experiment. All kinematics are parallel and the incident electron energy amounts to 4 GeV.

Kin	E	Q^2	E'	T_p	θ_e	θ_p
	[GeV]	[$(GeV/c)^2$]	[GeV]	[GeV]	[degr]	[degr]
1	4.0	0.8	3.57	0.43	13.59	-57.91
2	4.0	1.5	3.20	0.80	19.70	-47.58
3	4.0	3.0	2.40	1.60	32.46	-33.13
4	4.0	4.0	1.87	2.13	42.91	-25.80

Table 2. Single-arm counting rates, coincidence rate N_C and the real-to accidental coincidence ratio R/A for the proposed kinematics. A coincidence timing resolution of 2 ns and a duty factor of 100 % have been assumed in the calculation of R/A.

Kin	$N(e,e')$	$N(e,\pi^-)$	$N(e,p)$	$N(e,\pi^+)$	N_C	R/A
	[Hz]	[Hz]	[Hz]	[Hz]	[hour-1]	
1	3.9×10^5	3.1×10^4	4.2×10^4	2.5×10^4	1.6×10^7	86
2	2.2×10^4	1.0×10^4	5.9×10^3	2.1×10^3	3.6×10^6	2800
3	560	4.5×10^3	1.9×10^4	4.5×10^3	3.0×10^5	3170
4	90	5.9×10^3	1.1×10^4	1.9×10^3	5.4×10^4	6480

Table 3. Assumed polarimeter parameters. The quoted polarization components are calculated in plane-wave impulse approximation.

Kin	Anal. thickness [cm]	$A_y^2 f$ [$\times 10^3$]	D_{ll}	D_{lt}	$D_{ll}\sin(\chi)$
1	20	9.3	0.161	-0.126	0.143
2	30	10.9	0.304	-0.165	0.155
3	45	4.8	0.580	-0.212	-0.358
4	60	3.2	0.739	-0.233	-0.734

Table 4. Estimate for counting times. For the longitudinal polarization of the incident electrons we assume 40 %.

Kin	E [GeV]	Q^2 [$(GeV/c)^2$]	Time [Hours]
1	4.0	0.8	24
2	4.0	1.5	24
3	4.0	3.0	96
4	4.0	4.0	96

Table 5. Beam time request.

	Time [hours]
Setup and Checkout	50
Data Acquisition	240
TOTAL	290

References

1. G. van der Steenhoven *et al.*, Phys. Rev. Lett. **57**, 182 (1986); **58**, 1727 (1987).
2. D. Reffay-Pikeroen *et al.*, Phys. Rev. Lett. **60**, 776 (1988).
3. P.E. Ulmer *et al.*, Phys. Rev. Lett. **59**, 2259 (1987).
4. J.M. Laget in *"Modern Topics in Electron Scattering"*, Eds. B. Frois and I. Sick, World Scientific, p. 290 (1992); A. Magnon *et al.*, Phys. Lett. **222B**, 352 (1989).
5. T.D. Cohen *et al.*, Phys. Rev. Lett. **59**, 1276 (1987).
6. T. Suzuki, Phys. Rev. C **37**, 549 (1988).
7. M. Kohno, Phys. Rev. C **38**, 584 (1988).
8. L.S. Celenza *et al.*, Phys. Rev. Lett. **53**, 892 (1984).
9. P.J. Mulders, Phys. Rev. Lett. **54**, 2560 (1985).
10. G van der Steenhoven *et al.*, Phys. Lett. B **191**, 227 (1987).
11. K.A. Dow, MIT Ph-D thesis, (1987).
12. K. von Reden *et al.*, private communications.
13. Z.E. Meziani *et al.*, Phys. Rev. Lett. **54**, 1233 (1985).
14. P. Barreau *et al.*, Nucl. Phys. **A402**, 515 (1983).
15. C. Marchand *et al.*, Phys. Lett. **153B**, 29 (1985).
16. S. Krewald, Phys. Lett. **222B**, 338 (1989).
17. S. Boffi *et al.*, Nucl. Phys. **A386**, 599 (1982).
18. A. Picklesimer *et al.*, Phys. Rev. **C32**, 1312 (1985).
19. T.D. Cohen *et al.*, Phys. Rev. Lett. **59**, 1267 (1987).
20. R. Schiavilla *et al.*, Nucl. Phys. **A449**, 219 (1986).
21. Y. Akaishi, Nucl. Phys. **A416**, 409c (1984).
22. J.F.J. van den Brand *et al.*, Phys. Rev. Lett. **60**, 2006 (1988).
23. J.F.J. van den Brand *et al.*, Phys. Rev. Lett. **66**, 409 (1991).
24. J.F.J. van den Brand *et al.*, Nucl. Phys. **A534**, 637 (1991).
25. J.M. Laget, Phys. Lett. **199B**, 493 (1987).
26. R.G. Arnold *et al.*, Phys. Rev. **23**, 363 (1981).
27. R. Schiavilla, Phys. Rev. Lett. **65**, 835 (1990). **A449**, 219 (1986).
28. J.M. Laget, Phys. Lett. **151B**, 325 (1985).
29. J.M. Laget, Nucl. Phys. **A497**, 391c (1989).
30. J.M. Laget, Contribution to: "IX International Seminar on High Energy Physics Problems", Dubna (URSS), 14 - 19 June, 1988.
31. F.P. Juster *et al.*, Phys. Rev. Lett. **55**, 2261 (1985).
32. J.M. Laget, private communications.

33. J.S. McCarthy *et al.*, Phys. Rev. **C15**, 1396 (1979).
34. Conceptual Design Report, Basic Experimental Equipment, CEBAF(1990).
35. T. De Forest, Nucl. Phys. **A392**, 232 (1983).
36. J.S. O'Connell and J. Lightbody, Program EPC (1986).